Revista Mexicana de Astronomía y Astrofísica, **38**, 233–249 (2002)

A LOSSY METHOD FOR COMPRESSING RAW CCD IMAGES

Alan M. Watson

Instituto de Astronomía
Universidad Nacional Autónoma de México, Campus Morelia, México

Received 2002 June 3; accepted 2002 August 7

RESUMEN

Se presenta un método para comprimir las imágenes en bruto de dispositivos como los CCD. El método es muy sencillo: cuantización con pérdida y luego compresión sin pérdida con herramientas de uso general como gzip o bzip2. Se convierten los archivos comprimidos a archivos de FITS descomprimiéndolos con gunzip o bunzip2, lo cual es una ventaja importante en la distribución de datos comprimidos. El grado de cuantización se elige para eliminar los bits de bajo orden, los cuales sobre-muestrean el ruido, no proporcionan información, y son difíciles o imposibles de comprimir. El método es con pérdida, pero proporciona ciertas garantías sobre la diferencia absoluta máxima, la diferencia RMS y la diferencia promedio entre la imagen comprimida y la imagen original; tales garantías implican que el método es adecuado para comprimir imágenes en bruto. El método produce imágenes comprimidas de 1/5 del tamaño de las imágenes originales cuando se cuantizan imágenes en las que ningún valor cambia más de 1/2 de la desviación estándar del fondo. Esta es una mejora importante con respecto a las razones de compresión producidas por métodos sin pérdida, y aparentemente las imágenes comprimidas con bzip2 no exceden el límite teórico por más de unas decenas de por ciento.

ABSTRACT

This paper describes a lossy method for compressing raw images produced by CCDs or similar devices. The method is very simple: lossy quantization followed by lossless compression using general-purpose compression tools such as gzip and bzip2. A key feature of the method is that compressed images can be converted to FITS files simply by decompressing with gunzip or bunzip2, and this is a significant advantage for distributing compressed files. The degree of quantization is chosen to eliminate low-order bits that over-sample the noise, contain no information, and are difficult or impossible to compress. The method is lossy but gives guarantees on the maximum absolute difference, the expected mean difference, and the expected RMS difference between the compressed and original images; these guarantees make it suitable for use on raw images. The method consistently compresses images to roughly 1/5 of their original size with a quantization such that no value changes by more than 1/2 of a standard deviation in the background. This is a dramatic improvement on lossless compression. It appears that bzip2 compresses the quantized images to within a few tens of percent of the theoretical limit.

Key Words: **TECHNIQUES: IMAGE PROCESSING**

1. INTRODUCTION

Optical and infrared instruments now routinely produce huge amounts of image data. The largest current common-user CCD mosaic has 12k × 8k pixels (Veillet 1998); a single image from such a mosaic is 192 MB in size. The largest current common-user infrared detector mosaic has 2k × 2k pixels (Beckett et al. 1998), but makes up for its smaller size by being read more frequently. More than a few nights of data from such instruments can easily overwhelm workstation-class computers. Compression is a solution to some of the problems generated by these large quantities of data. Similarly, compression can improve the effective bandwidth to remote observatories (in particular space observatories), remote data archives, and even local storage devices.

This paper describes in detail a lossy method for compressing raw images and presents a quantitative comparison to other lossy methods. It is organized as follows: § 2 reviews the limitation of lossless compression and the motivation for lossy compression; § 3 briefly summarizes the most relevant previous work on lossy compression; § 4 describes the new method; § 5 presents results on the distribution of differences between the original and compressed images; § 6 investigates the performance of the method with particular reference to hcomp; § 7 compares the performance of the method to other similar methods; § 8 discusses the suitability of the method for compressing raw data and investigates some consequences of such use; § 9 discusses how the method might be improved; and § 10 presents a brief summary.

2. LOSSLESS COMPRESSION

2.1. *The Shannon Limit*

Compression methods can be classified as lossless or lossy depending on whether compression changes the values of the pixels. The difficulties of lossless compression of CCD images have been discussed by White (1992), Press (1992), and Véran & Wright (1994). The noise in images from an ideal CCD consists of Poisson noise from the signal and uncorrelated Gaussian read noise. If the signal is measured in electrons, the variance of the Poisson noise is equal to the signal and the variance of the read noise is typically 10–100. However, CCD images are often quantized to sample the read noise, with typical analog-to-digital converter gains being 1–5 electrons. This means that the larger noises associated with larger signal levels can be hugely over-sampled. If this is the case, the low-order bits in an image are essentially uniform white noise, contain no information, and cannot be compressed.

To illustrate this, series of $512 \times 512 \times 16$-bit FITS images of pure Gaussian noise were created. The images were written with with a BSCALE of $q\sigma$, so the standard deviation is sampled by a factor of $1/q$. Shannon's first theorem (Shannon 1948ab, 1949) allows us to calculate the optimal compression ratio for these images. The theorem states that if a stream of bits is divided into fixed-length "input code units", then the minimum number of bits required to encode each input code unit is just the Shannon entropy,

$$H \equiv -\sum_{\forall p_i \neq 0} p_i \log_2 p_i, \tag{1}$$

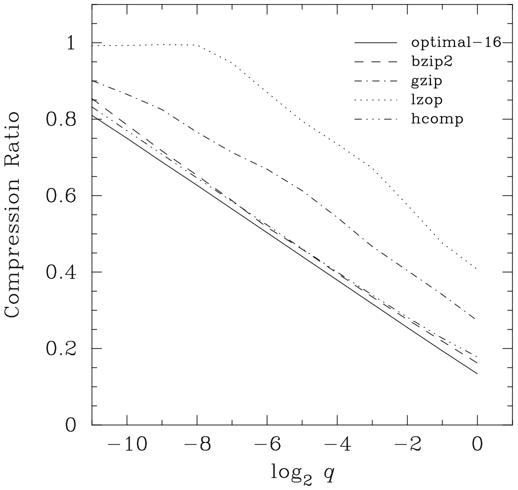

Fig. 1. The compression ratio (ratio of compressed size to original size) as a function of $\log_2 q$ for an image consisting of pure Gaussian noise with standard deviation σ written as a 16-bit FITS image with a BSCALE of $q\sigma$ and then losslessly compressed. The solid line is the Shannon limit for optimal compression of the individual 16-bit pixels and the other lines show the ratios achieved by bzip2, gzip, lzop, and hcomp (used losslessly).

where p_i is the normalized frequency of the input code unit i. From this we can derive that the optimal input code unit is the longest one for which the bits are still correlated; since in this case, each pixel is independent, the optimal input code unit is simply a 16-bit pixel. The resulting optimal compression ratio (the ratio of the compressed size to original size) will be $H/16$.

Figure 1 shows as a function of q the optimal compression ratio determined by calculating the Shannon entropy explicitly. As can be seen, the optimal compression ratio is a constant minus $(\log_2 q)/16$. Intuitively, this is expected: the number of incompressible low-order bits grows as $-\log_2 q$ and the fraction of the compressed image occupied by these bits grows as $-(\log_2 q)/16$. This result is not new; Romeo et al. (1999) investigated the Shannon limit for compression of a quantized Gaussian distribution, and their equation (3.3), in my notation, is

$$H \approx \log_2 \sqrt{2\pi e} - \log_2 q, \tag{2}$$

This equation was derived in the limit of small q, but Gaztañaga et al. (2001) have shown that the corrections for finite q are small for q at least as large as 1.5. Not surprisingly, the Shannon entropies and compression ratios calculated using this equation and calculated explicitly for the Gaussian noise images are in almost perfect agreement.

Real astronomical images contain information in addition to noise, but nevertheless this exercise demonstrates the futility of attempting to achieve good compression ratios for images that contain over-sampled noise. For example, if the noise is over-sampled by a factor of 60 (which corresponds to $q = 60$), it is *impossible* to compress the image losslessly to better than half its size; too much of the image is occupied by white noise in the low-order bits. This exercise also explains why lossless methods are often more successful on images with low signals, such as biases or short exposures, and less successful on images with high signals, such as flats, deep exposures, and infrared images.

We are forced to the conclusion that if we wish to significantly and consistently compress raw images, including those with high background levels, there is no alternative but to use lossy compression methods.[1]

2.2. *Real Lossless Compression Methods*

The Shannon limit is a theoretical limit and is independent of any particular real compression method. Nevertheless, it is useful to consider how well real lossless compression methods perform on Gaussian noise both to introduce these methods and to investigate how well they perform in this idealized case. The methods considered are Huffman coding, Arithmetic coding, hcomp, bzip2, gzip, and lzop.

Huffman coding (Huffman 1952; Press et al. 1992, § 20.4) and Arithmetic coding (Whitten, Neal, & Cleary 1987; Press et al. 1992, § 20.5) make use of the frequency distribution of fixed input code units. As such, if 16-bit pixel values are taken as the input code unit, the compression ratio should be close to the Shannon limit (provided the image is large compared to the frequency table). Indeed, Gaztañaga et al. (2001) show that Huffman coding of quantized Gaussian noise is very nearly optimal for $q \leq 1$ (see their Figure 1). For this reason, we need not investigate actual implementations of these methods but instead can approximate their compression ratios by the Shannon limit.

Hcomp (White 1992) is specialized to compressing 16-bit astronomical images and uses a complex algorithm based on a wavelet transformation of the pixel values, optional quantization of the coefficients, and quad-tree compression of the coefficients. Hcomp can be used losslessly by omitting the quantization of the coefficients.

Bzip2 (Seward 1998), gzip (Gailly 1993), and lzop (Oberhumer 1998) are methods for compressing general byte streams and use dictionary-based algorithms with variable-length input code units. They are portable, efficient, and free from patents. Sources and executables are freely available. They represent different trade-offs between compression ratio and speed, with bzip2 typically being slowest but achieving the best compression ratios, lzop typically being the fastest but achieving the worst compression ratios, and gzip being intermediate in both speed and compression ratio.

Fig. 1 shows the compression ratio achieved by hcomp (used losslessly), bzip2, gzip, and lzop. The compression ratios have the same trend as the Shannon limit—they also cannot compress white noise in the low order bits—but the constant is larger. (Lzop is a slight exception in that it is initially unable to compress the image but then follows the expected trend.) Both bzip2 and hcomp are quite close to the Shannon limit. The surprisingly good performance of bzip2 suggests that it might be useful in compressing images; a large portion of the rest of this paper will be devoted to evaluating this suggestion.

3. PRIOR WORK ON LOSSY COMPRESSION

Louys et al. (1999) have recently scrutinized lossy compression methods, including hcomp (White 1992). Their investigation concentrated on relatively high compression of reduced images. Compressing raw images is somewhat different, in that we wish to maintain all of the information in the image and avoid introducing spurious features. Even weak features can be important, as subsequent co-addition, spatial filtering, or other processing may increase their significance. Therefore, for raw images we require methods that suppress only those parts of an image that contains no information (the white noise in the low-order bits) and preserve perfectly those parts that do contain information (the mid-order and high-order bits). None of the lossy methods considered by Louys et al. (1999) can give this guarantee. For raw images, we must consider other methods.

[1] The results of White & Becker (1998) appear to contradict this statement. These authors achieve compression ratios of 17%–32% on four WFPC2 images using lossless Rice compression. However, WFPC2 images have low backgrounds, due to the small pixels of WFPC2 and low sky brightness in orbit, and the gain normally under-samples the read noise. It is likely that none of their images has a large white noise component, and as such their sample of images is not representative of the full range of raw astronomical images.

More promising is the work of White & Greenfield (1999), Nieto-Santisteban et al. (1999), and Gaztañaga et al. (2001). These authors have all presented lossy compression methods that work by discarding white noise and then using a lossless compression method. White & Greenfield (1999) discard white noise from generic floating-point images by quantizing each row by a fraction of the estimated noise and converting to integers, Nieto-Santisteban et al. (1999) discard white noise from simulated NGST data by scaling and taking the square root, and Gaztañaga et al. (2001) discard white noise from simulated data from cosmic microwave background experiments by quantizing by a fraction of the standard deviation. White & Greenfield (1999) and Nieto-Santisteban et al. (1999) use the Rice compression algorithm (Rice, Yeh, & Miller 1993) and Gaztañaga et al. (2001) use Huffmann coding (Huffman 1952; see Press et al. 1992, § 20.4).

Comparisons to the work of White & Greenfield (1999) and Nieto-Santisteban et al. (1999) are made in § 7; the method suggested by Gaztañaga et al. (2001) is very similar to the one suggested here, but has a completely different context.

4. METHOD

The quantization compression method is so simple that it is somewhat embarrassing to describe it as a "method". It consists of lossy quantization (or resampling) in brightness of the original image to produce a quantized image, followed by lossless compression of the quantized image. Decompression consists of reversing the lossless compression to recover the quantized image. The resampling quantum will normally be a specified fraction of the expected noise in the background. The aim of quantization is to reduce the over-sampling of the noise, reduce the number of bits of white noise, and permit the lossless compression method to perform better. The quantization method is intended to be used on raw data from CCD-like devices.

4.1. *Quantization*

The first stage of the quantization method is to produce a quantized image. For definiteness, the quantization is described in terms of integer FITS images (Wells, Greisen, & Harten 1981). This is the most common format for archived raw data. The extension to other image formats is obvious.

Each integer n in the original FITS image is related to a data value b by

$$b = b_{\rm zero} + n b_{\rm scale}, \tag{3}$$

where $b_{\rm zero}$ and $b_{\rm scale}$ are taken from the BZERO and BSCALE records in the FITS header and have defaults of 0 and 1. The data quantum Q_b is chose to be an integral multiple Q_n of $b_{\rm scale}$. The quantized brightness $\hat{b}$ is thus

$$\hat{b} = b_{\rm zero} + Q_b [b/Q_b] b_{\rm scale}. \tag{4}$$

Here, $[x]$ is the nearest integer to x with half integers rounded to the nearest even integer to help avoid biases. The quantized image is written with the same BZERO and BSCALE values as the original image. Thus, the quantized integer $\hat{n}$ in the quantized FITS file is related to the quantized data value $\hat{b}$ by

$$\hat{n} = (\hat{b} - b_{\rm zero})/b_{\rm scale}. \tag{5}$$

It can be seen that this quantization can be carried out entirely in integer arithmetic as

$$\hat{n} = Q_n [n/Q_n]. \tag{6}$$

Certain values in the original image are special and are treated accordingly. Thus, "blank" pixels (those which have the value specified by the BLANK record in the FITS header) are not changed and any pixel whose quantized value would be the blank value is not changed. The values corresponding to the maximum and minimum integer values are treated similarly, as these values are often used to flag saturated data or implicitly blank pixels. (Some images have ancillary information, such as the exposure time and engineering information, encoded in "data" pixels; this information should be transferred to the header prior to compression.)

The quantum Q_b should be determined according to the noise model for the detector. For CCD-like devices, the estimated standard deviation σ_b of the noise is given by

$$\sigma_b = \begin{cases} ((b - b_{\rm bias})g + r^2)^{1/2}/g & b > b_{\rm bias} \\ r/g & b \le b_{\rm bias} \end{cases}. \tag{7}$$

Here g is the gain in electrons, r is the read noise in electrons, and $b_{\rm bias}$ is the bias level. We first determine the bias level $b_{\rm bias}$ and data background level $b_{\rm data}$ in the image, perhaps from the mean, median, or mode in certain regions, and hence the noise by applying Equation (7). We then determine the quantum as

$$Q_b = \begin{cases} b_{\rm scale} \lfloor q\sigma_b / b_{\rm scale} \rfloor & q\sigma_b > b_{\rm scale} \\ b_{\rm scale} & q\sigma_b \le b_{\rm scale} \end{cases}, \tag{8}$$

or

$$Q_n = \begin{cases} \lfloor q\sigma_b / b_{\rm scale} \rfloor & q\sigma_b > b_{\rm scale} \\ 1 & q\sigma_b \le b_{\rm scale} \end{cases}. \tag{9}$$

Here $\lfloor x \rfloor$ is the largest integer no greater than x. Thus, the parameter q controls the coarseness of the quantization by setting the size of the quantum Q_b to be the smallest integer multiple of $b_{\rm scale}$ no larger than q times the noise. Suitable values for q are 0.5 to 2 (see § 5 and § 6).

There is no requirement that the quanta be equal over the entire image. The data and overscan regions of an image should probably be quantized with different quanta as they likely have different characteristic noises. Furthermore, if the background and hence the noise vary significantly within the data region, it makes sense to subdivide the data region and use different quanta within each subregion. However, it is important the quanta are constant within regions and are not determined on a pixel-to-pixel basis, as this can introduce small but nevertheless real biases (see § 7).

4.2. *Compression*

The quantized FITS file is no smaller than the original FITS file. Therefore, the second stage of the quantization method is to compress the quantized FITS file using a lossless compression method. The methods investigated here are bzip2 (Seward 1998), gzip (Gailly 1993), lzop (Oberhumer 1998), and hcomp (White 1992). Hypothetical optimal 16-bit and 32-bit encoders (which will approximate Huffman or Arithmetic encoders) are also considered.

4.3. *Decompression*

The quantized image is recovered as a standard FITS file by reversing the lossless compression using bunzip2, gunzip, lzop, or hdecomp.

5. DISTRIBUTION OF DIFFERENCES

One advantage of the simplicity of the quantization method is that we can derive useful information on the distribution of the differences between the quantized and original images. These give the confidence required to apply the quantization method to raw data. Note that the distribution of differences is determined only by the quantization stage; the compression stage is lossless.

We define the normalized difference Δ between the quantized and original data values to be

$$\Delta = \frac{\hat{b} - b}{\sigma_b} \ . \qquad (10)$$

A firm upper bound on the magnitude of Δ is

$$|\Delta| \le \frac{Q_b}{2\sigma_b} \le 0.5q. \qquad (11)$$

Thus, no difference is larger in magnitude than $q/2$ standard deviations in the background. Provided q is not larger than 2, we expect Δ to be roughly uniformly distributed about zero (on discrete points corresponding to integer multiples of $b_{\rm scale}/\sigma_b$) and so we expect the mean and standard deviation of Δ (the mean and RMS normalized difference) to be approximately

$$\mu_\Delta \approx 0 \ , \qquad (12)$$

and

$$\sigma_\Delta \approx \frac{q}{\sqrt{12}} \approx 0.29q \ . \qquad (13)$$

The quantity σ_Δ corresponds to the square-root of the "digital distortion" $\mathcal{D}$ discussed by Gaztañaga et al. (2001). They show that a quantization of a distribution of standard deviation σ_b will result in a distribution with a standard deviation $\sigma_{\hat{b}}$ given by

$$\frac{\sigma_{\hat{b}}}{\sigma_b} \approx \sqrt{1 + \frac{q^2}{12}} \approx 1 + 0.042q \ ,$$

which comes from adding the variances in quadrature and assuming that the difference $\hat{b} - b$ is uncorrelated with b (which is a good approximation provided q is small).

6. PERFORMANCE

This section presents tests and comparisons of the performance of the quantization compression method proposed here, qcomp, in terms of the distribution of differences, compression ratio, and speed of compression and decompression. Hcomp and optimal 16-bit and 32-bit encoders serve as points of reference.

6.1. *Trial Images*

Five trial images were selected to sample different noise regimes and scenes. The images were obtained with a CCD at the Observatorio Astronómico Nacional at Sierra San Pedro Mártir and saved as 512 × 512 × 16-bit FITS files with a BSCALE of 1. The images were (a) a bias exposure, (b) a shallow exposure of a sparse field (a standard star), (c) a deep exposure of a relatively sparse field (a small galaxy), (d) a deep exposure of a complex field (a nebula), and (e) a flat-field exposure. To make the

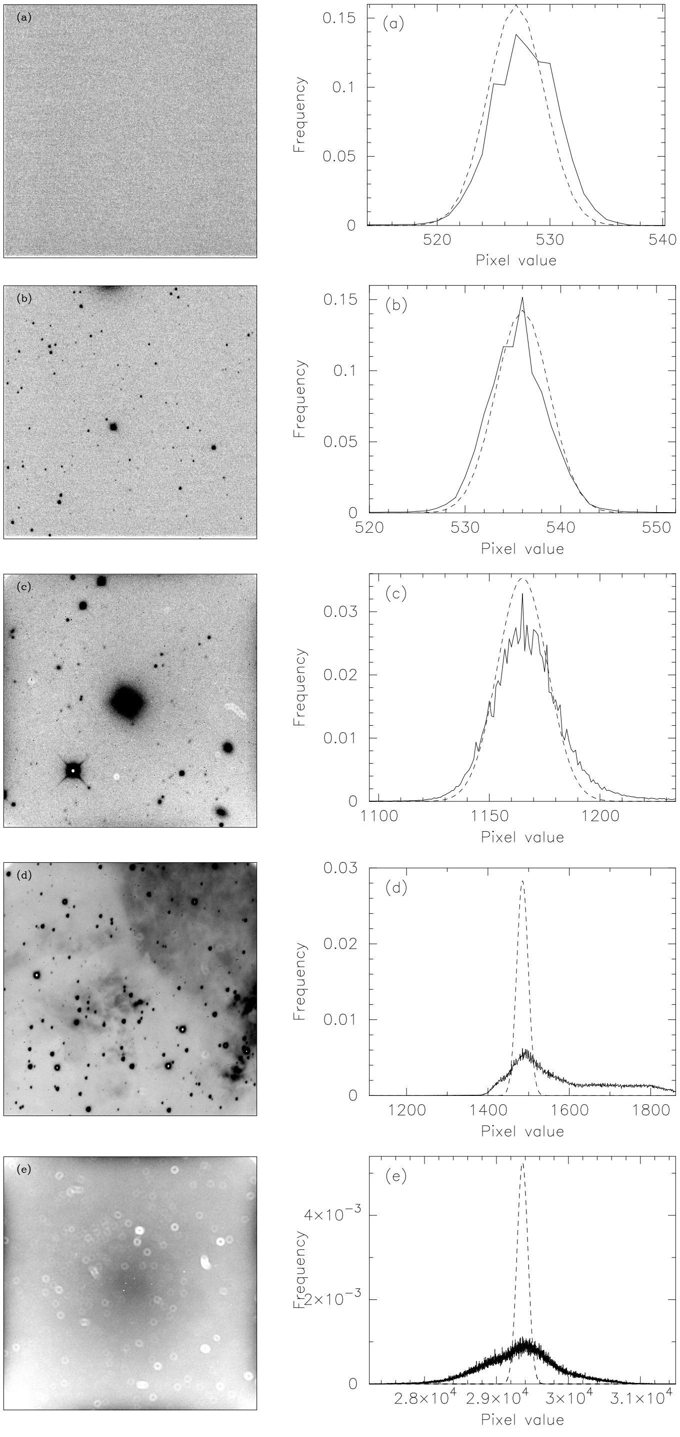

Fig. 2. The trial images. The images in the left panels are stretched from $-2\hat{\sigma}_b$ to $+6\hat{\sigma}_b$ about the mode and the histograms in the right panels are shown stretched from $-4\hat{\sigma}_b$ to $+4\hat{\sigma}_b$ about the mode, where $\hat{\sigma}_b$ is the standard deviation of the pixel values (after 5σ clipping). In the histograms, the solid line is the observed distribution of pixel values and the dashed line is the expected contribution from noise. The real distributions are significantly broader than the noise in image in image (d) because of structure in the scene and in image (e) because of structure in the flat field, both at low frequencies and on a pixel-to-pixel basis.

TABLE 1

TEST IMAGES

Image	Description	σ_b	$\hat{\sigma}$
(a)	Bias	2.5	3.3
(b)	Shallow sparse field	2.8	4.0
(c)	Deep sparse field	11.3	17.4
(d)	Deep complex field	14.1	94.1
(e)	Flat field	76.0	532.0

comparison with hcomp fair, the overscan sections were removed, as hcomp does not distinguish between the data and overscan sections.

The bias and background levels in each image were estimated from the mode in the exposed and overscan regions, and the noise σ_b estimated by applying equation (7). The standard deviation $\hat{\sigma}_b$ of the pixel values was also determined (with 5σ clipping). Figure 2 shows the images and the histograms of the pixel values, along with the expected contribution to the histogram width from the noise. The histograms of the images (a), (b), and (c) are dominated by noise. However, the histogram of image (d) is much wider than the noise because of structure in the scene and the histogram of image (e) is much wider because of structure in the flat field (large-scale structure of around 1.5% and pixel-to-pixel variations of around 0.5%).

Any choice of trial images is likely to be somewhat arbitrary. However, one advantage of these images is that they cover a good range of noise regimes and scenes. This implies that if a compression method can produce good results for all of the trial images, it is likely to produce good results for other sets of images, regardless of the relative frequency of each type of image. Thus, we see that a successful compression method must achieve not only a good mean compression ratio for the whole set of trial images but also consistently good compression ratios for each individual image.

6.2. *Compression*

The images were compressed using the following methods:

1. Lossless compression by hcomp with the “-s 0” option.
2. Lossless compression using hypothetical optimal 16-bit and 32-bit methods. The compression ratios for these methods were determined by calculating the Shannon entropy for each image, given by equation (1). Although these methods are hypothetical, they will approximate Huffman and Arithmetic coding.
3. Lossless compression by direct application of bzip2, gzip, and lzop with options varying from “-1” (fastest/worst) to “-9” (slowest/best).
4. Lossy compression using hcomp, with the degree of loss being controlled by value of the “-s” option. The value of this option was $2q\sigma_b$, which gives roughly the same RMS difference as the quantization method with the same value of q.
5. Lossy compression using the quantization method described in § 4 implemented by the program qcomp (available from the author), with hypothetical optimal 16-bit and 32-bit compression, bzip2, gzip, lzop, and lossless hcomp used for the actual compression stage.

The distributions of differences, compression ratios, and speeds are shown in Tables 2 and 3 and Figures 3 and 4. The lossy methods are shown for q values of 0.5, 1, 2, 4, 8, and 16. Table 2 and Figure 3 show the RMS, maximum absolute, and mean normalized difference Δ between the compressed and original images. [The normalization is to σ_b, the noise in the image; see Equation (10).] Obviously, the lossless methods do not appear as their differences are uniformly zero. Table 3 shows the compression ratio achieved for each image (the ratio of the compressed size to original size), the mean compression ratio for all five images, and the speed at which the five images were compressed and decompressed. These speeds were measured on a computer with a single 1.9 GHz Pentium IV processor. Speeds are not given for the optimal 16-bit and 32-bit methods, as these methods are hypothetical.

The compression speeds quoted in Table 3 do not include the time taken to determine the background level and calculate the noise. Determining these using the mean, median, or mode proceeds at about 11 Mpixel/s and reduces the compression speeds to 0.79 Mpixel/s for qcomp/bzip2 (9% slower), 2.84 Mpixel/s for qcomp/gzip (26% slower), 4.03 Mpixel/s for qcomp/lzop (37% slower), 1.47 Mpixel/s for qcomp/hcomp (13% slower), and 1.94 Mpixel/s for hcomp (18% slower) for $q = 1$.

Figure 4 shows q, the RMS difference, and maximum absolute differences as functions of the compression ratio for the more effective lossy compression methods.

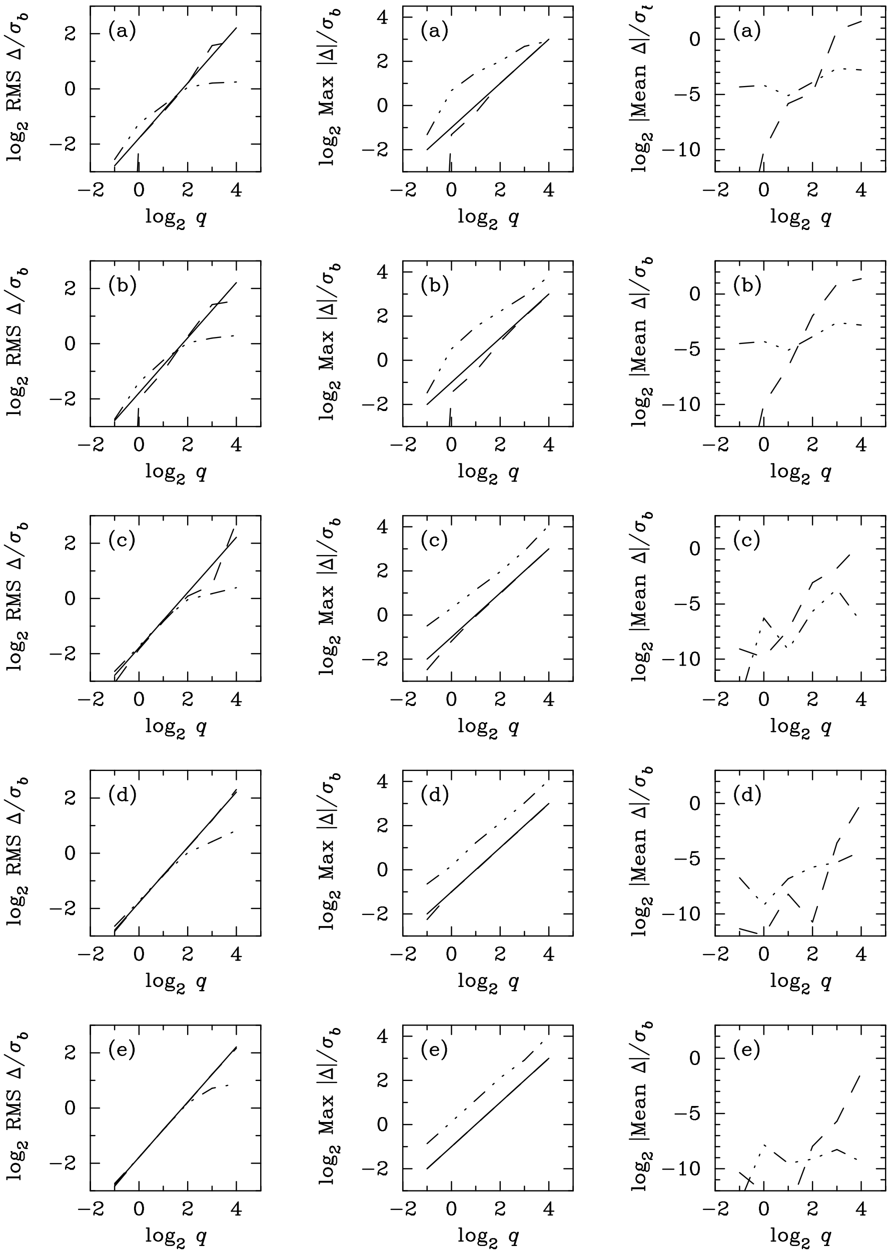

Fig. 3. The RMS, maximum absolute, and mean differences between the compressed and original images as functions of q for the four images (a)–(e) for qcomp (dashed lines) and hcomp (dotted-dashed lines). The solid lines show the relations predicted for qcomp in § 5.

TABLE 2

DISTRIBUTIONS OF DIFFERENCES

q	Method	RMS, Maximum Absolute, and Mean Differences Δ in units of σ_b				
		(a)	(b)	(c)	(d)	(e)
0.5	qcomp	0.00/0.00/+0.00	0.00/0.00/+0.00	0.12/0.18/+0.00	0.14/0.21/−0.00	0.14/0.25/−0.00
	hcomp	0.17/0.40/+0.05	0.15/0.36/+0.04	0.16/0.71/−0.00	0.16/0.64/+0.01	0.15/0.55/+0.00
1	qcomp	0.29/0.40/−0.00	0.25/0.36/−0.00	0.28/0.44/+0.00	0.29/0.50/−0.00	0.29/0.50/−0.00
	hcomp	0.42/1.60/−0.06	0.38/1.43/−0.05	0.30/1.24/+0.01	0.30/1.13/−0.00	0.29/1.09/−0.00
2	qcomp	0.56/0.80/+0.02	0.50/0.71/+0.01	0.56/0.97/+0.00	0.57/0.99/+0.00	0.58/1.00/+0.00
	hcomp	0.66/2.80/+0.03	0.66/2.86/−0.03	0.58/2.21/+0.00	0.58/2.34/−0.01	0.58/2.16/−0.00
4	qcomp	1.14/2.00/−0.03	1.20/1.79/−0.25	1.06/1.95/−0.12	1.15/1.99/+0.00	1.15/2.00/+0.00
	hcomp	1.04/4.00/−0.07	1.02/4.64/−0.07	0.97/3.89/−0.02	1.01/4.33/−0.02	1.13/4.33/−0.00
8	qcomp	2.97/4.00/+1.74	2.67/3.93/+1.85	1.40/3.98/−0.29	2.29/3.97/+0.08	2.34/4.00/+0.02
	hcomp	1.16/6.40/−0.16	1.15/7.50/−0.17	1.13/7.52/−0.08	1.34/8.16/−0.02	1.64/7.57/−0.00
16	qcomp	3.34/8.00/+3.06	2.95/7.86/+2.61	6.85/7.96/+1.47	4.95/7.94/−1.01	4.48/8.00/+0.41
	hcomp	1.19/7.60/−0.15	1.23/13.9/−0.14	1.31/16.7/−0.01	1.77/16.7/−0.05	1.84/16.3/−0.02

6.3. *Lossless Methods*

The upper section of Table 3 gives the compression ratios for the lossless methods. The best methods are hcomp, bzip2, and the optimal 16-bit and 32-bit methods, which achieve mean compression ratios of about 0.4.

In contrast to the compression of pure Gaussian noise discussed in § 2, hcomp and bzip2 achieve better mean compression ratios than the optimal 16-bit method. How can this be? The explanation is that in the deep and flat-field images, (c), (d), and (e), there are correlations between adjacent pixels that both hcomp and bzip2 can exploit—hcomp because its wavelets can extend over more than one pixel and bzip2 because it can increase the size of its input code unit to cover more than one pixel. This also explains why the optimal 32-bit method, which considers pixel in pairs, performs better than the optimal 16-bit method, which considers pixels individually. However, in the bias and shallow images, (a) and (b), the noise component is dominant, and the optimal 16-bit method performs slightly better than hcomp and bzip2, just as for pure Gaussian noise. The optimal 32-bit method performs slightly better than the optimal 16-bit method even for the bias image, which suggests that there are small pixel-to-pixel correlations even in this image, presumably due to the bias structure. (Another way of looking at this is that optimal 16-bit compression uses only the histogram of pixel values whereas the other methods use both the histogram and, to varying degrees, the image; the image adds information on correlations between pixels, and allows for more efficient compression.)

Nevertheless, the mean compression ratio of about 0.4 masks variations of factors of 2–3 in the compression ratio for individual images, with the bias and shallow images, (a) and (b), being compressed well to about 0.25 and the deep and flat-field images, (c), (d), and (e), being compressed poorly to 0.4–0.7. This is as expected; the bias and shallow images compress well as their noises are only moderately over-sampled, but the deep and flat-field images compress badly as their noises are significantly over-sampled. In short, the lossless methods produce inconsistent results, and while they will compress some sets of data very well (for example, those dominated by observations of standard stars or images in low-background narrow-band filters), they will compress others very poorly (for example, those dominated by deep images with high backgrounds). In all, these results confirm what we already knew: if we want to achieve consistently good compression ratios, we have no choice but to adopt lossy methods.

(Table 3 also shows the effect of the options to bzip, gzip, and lzop. For bzip2 and gzip there is not much improvement in the compression ratio between the “-1” and “-9” options, but the compression speed drops noticeably. For lzop there is a significant improvement, but the compression speed

TABLE 3

COMPRESSION RATIOS AND SPEEDS

q	Method	Compression Ratio						Compression	Decompression
		(a)	(b)	(c)	(d)	(e)	mean	Mpixel/s	Mpixel/s
				Lossless methods					
0	hcomp	0.253	0.266	0.391	0.440	0.591	0.388	2.06	2.04
	optimal-16	0.232	0.246	0.395	0.561	0.692	0.425		
	optimal-32	0.225	0.236	0.372	0.466	0.525	0.365		
	bzip2 -1	0.242	0.256	0.393	0.460	0.634	0.397	0.73	2.07
	bzip2 -9	0.241	0.254	0.388	0.449	0.620	0.390	0.58	1.52
	gzip -1	0.329	0.343	0.502	0.641	0.769	0.517	2.81	10.20
	gzip -9	0.296	0.313	0.488	0.621	0.766	0.497	0.36	11.49
	lzop -1	0.498	0.509	0.709	0.828	0.992	0.707	9.80	34.48
	lzop -3	0.498	0.509	0.709	0.825	0.991	0.706	10.31	34.48
	lzop -7	0.383	0.396	0.567	0.691	0.877	0.583	0.60	32.26
	lzop -8	0.386	0.399	0.562	0.691	0.876	0.583	0.20	32.26
	lzop -9	0.387	0.399	0.562	0.691	0.876	0.583	0.16	32.26
				Lossy methods					
0.5	hcomp	0.235	0.249	0.234	0.260	0.262	0.248	2.20	2.23
	qcomp/optimal-16	0.233	0.246	0.254	0.389	0.369	0.298		
	qcomp/optimal-32	0.226	0.237	0.235	0.312	0.313	0.265		
	qcomp/bzip2	0.243	0.257	0.246	0.274	0.280	0.260	0.83	2.46
	qcomp/gzip	0.330	0.343	0.341	0.421	0.448	0.377	3.52	10.31
	qcomp/lzop	0.499	0.510	0.506	0.591	0.633	0.548	6.13	32.26
	qcomp/hcomp	0.256	0.269	0.389	0.441	0.576	0.386	1.68	2.03
1	hcomp	0.167	0.179	0.172	0.198	0.198	0.183	2.37	2.43
	qcomp/optimal-16	0.163	0.175	0.186	0.328	0.307	0.232		
	qcomp/optimal-32	0.156	0.166	0.168	0.253	0.253	0.199		
	qcomp/bzip2	0.176	0.189	0.176	0.209	0.214	0.193	0.85	2.62
	qcomp/gzip	0.259	0.271	0.268	0.352	0.373	0.305	3.83	11.90
	qcomp/lzop	0.442	0.450	0.447	0.499	0.519	0.471	6.37	32.26
	qcomp/hcomp	0.239	0.252	0.395	0.420	0.526	0.366	1.70	2.01
2	hcomp	0.098	0.104	0.108	0.133	0.133	0.115	2.53	2.64
	qcomp/optimal-16	0.099	0.111	0.130	0.267	0.246	0.171		
	qcomp/optimal-32	0.092	0.103	0.114	0.196	0.193	0.140		
	qcomp/bzip2	0.108	0.120	0.120	0.148	0.154	0.130	0.83	2.76
	qcomp/gzip	0.186	0.197	0.204	0.279	0.292	0.232	4.31	12.82
	qcomp/lzop	0.373	0.380	0.378	0.418	0.421	0.394	6.67	35.71
	qcomp/hcomp	0.247	0.262	0.364	0.360	0.456	0.338	1.68	1.98
4	hcomp	0.035	0.046	0.049	0.075	0.080	0.057	2.75	2.87
	qcomp/optimal-16	0.064	0.071	0.073	0.207	0.185	0.120		
	qcomp/optimal-32	0.057	0.063	0.059	0.146	0.139	0.093		
	qcomp/bzip2	0.070	0.075	0.063	0.097	0.101	0.081	0.53	3.37
	qcomp/gzip	0.137	0.144	0.122	0.203	0.185	0.158	5.13	15.15
	qcomp/lzop	0.285	0.304	0.212	0.322	0.346	0.294	7.25	37.04
	qcomp/hcomp	0.221	0.250	0.327	0.310	0.357	0.293	1.76	2.05
8	hcomp	0.005	0.011	0.020	0.036	0.020	0.018	2.85	3.05
	qcomp/optimal-16	0.052	0.044	0.033	0.150	0.128	0.081		
	qcomp/optimal-32	0.047	0.038	0.021	0.101	0.094	0.060		
	qcomp/bzip2	0.060	0.049	0.015	0.060	0.060	0.049	0.31	3.73
	qcomp/gzip	0.120	0.099	0.030	0.127	0.122	0.100	5.68	19.23
	qcomp/lzop	0.250	0.187	0.038	0.195	0.226	0.179	7.41	38.46
	qcomp/hcomp	0.217	0.241	0.088	0.239	0.295	0.216	1.84	2.07
16	hcomp	0.004	0.007	0.015	0.024	0.007	0.011	2.99	3.22
	qcomp/optimal-16	0.010	0.013	0.077	0.103	0.072	0.055		
	qcomp/optimal-32	0.005	0.008	0.068	0.070	0.051	0.040		
	qcomp/bzip2	0.002	0.004	0.072	0.041	0.030	0.030	0.40	3.51
	qcomp/gzip	0.007	0.011	0.140	0.083	0.061	0.060	5.52	16.67
	qcomp/lzop	0.007	0.012	0.291	0.128	0.105	0.109	7.46	38.46
	qcomp/hcomp	0.011	0.026	0.403	0.210	0.159	0.162	1.80	2.01

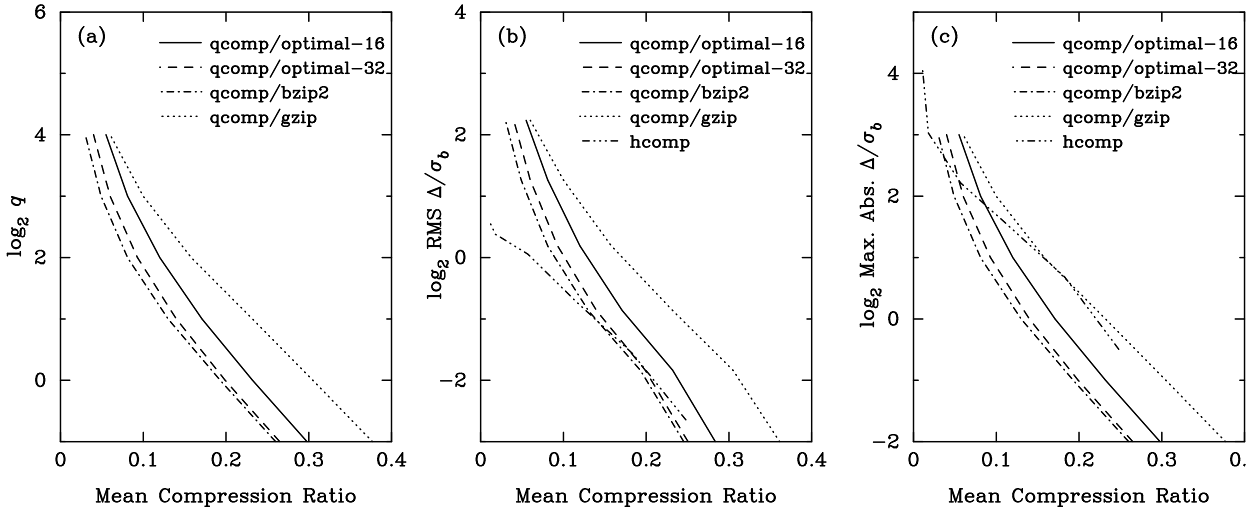

Fig. 4. The RMS and maximum absolute differences as functions of the mean compression ratio for the lossy compression methods. The solid line shows the Shannon entropy limit for $q \leq 1.5$.

drops precipitously. It seems clear that the "-1" option is preferable, and for this reason it was used in the lossless compression stage by qcomp.)

6.4. *Lossy Methods*

Table 2 and Figure 3 shows that the distributions of differences for qcomp are behaving much as predicted in § 5. For $q \leq 2$, the RMS difference is roughly $0.3q\sigma_b$, the maximum absolute difference is $0.5q\sigma_b$, and the mean difference is roughly zero. For larger values of q, the mean difference ceases to be close to zero, as might be expected when the quantization is too coarse to adequately sample both sides of a sharply-peaked distribution. This suggests that qcomp should not be used beyond $q \approx 2$.

Comparison of the distributions of differences for qcomp and hcomp in Figure 3 reveals two trends. First, for $q \leq 2$, the RMS differences are very similar. This is not surprising as the hcomp option was set to give this result. However, qcomp has lower values of the maximum absolute difference and mean difference. For larger values of q, the RMS differences and mean differences for hcomp are much better than those for qcomp.

Moving from the performance of the quantization step to the performance of the compression step, we first investigate what appears to be a worrying anomaly: when the bias image, (a), is quantized with $q = 1$, Table 3 shows that optimal 16-bit compression gives a compression ratio of 0.163, whereas equation 2 indicates that optimal 16-bit compression of quantized Gaussian noise with $q = 1$ should give a compression ratio of about 0.128. The bias image has very little structure and so should to a good approximation be simply Gaussian noise, so why are the compression ratios so different? Only a small part of the difference can be explained by corrections to equation 2 for finite q; numeric experiments give a true compression ratio for Gaussian noise with $q = 1$ of 0.134. The explanation for the remaining difference is that the noise σ_b in the bias image is 2.5 and is not an integer multiple of b_{scale}, and so the quantum $Q_b = b_{\mathrm{scale}}\lfloor q\sigma_b/b_{\mathrm{scale}}\rfloor$ is rounded down to 2. Thus, the proper comparison to compressing the bias image with $q = 1$ is compressing Gaussian noise with $q = 0.8$. By equation 2, this would have a compression ratio of 0.148, and numerical experiments give a value of 0.153, which is much closer to the 0.163 of the bias image. The remaining difference is presumably due to structure in the bias and non-Gaussian contributions to the noise (for example, the slightly flat top to the histogram in Figure 2a). Similarly, the shallow image (b) should be properly compared with Gaussian noise quantized with $q = 0.7$, which has a compression ratio of 0.162. The other images have large values of σ_b, so the truncation of Q_b does not effect them significantly.

Figure 4a shows the mean compression ratios achieved by qcomp/optimal-16, qcomp/optimal-32, qcomp/bzip2, and qcomp/gzip as functions of q. (Neither qcomp/lzop nor qcomp/hcomp are shown, as they are significantly worse.) The best mean compression ratios are achieved by qcomp/bzip2; again, bzip2 appears to be finding correlations between pixels that are not exploited by either the optimal 16-bit or 32-bit methods, especially in the cases of the deep image of the nebula (d) and the flat-field image (e). For $q = 1$ and $q = 2$ the mean compression ratios are 0.19 and 0.13, that is, factors of two and three better than lossless compression with bzip2. Furthermore, Table 3 shows that qcomp/bzip2 is achieving consistently good compression ratios which vary by only 20% from 0.176 to 0.214 for $q = 1$.

Appropriate figures of merit for comparing hcomp and qcomp/bzip2, are the RMS and maximum absolute difference at a given mean compression ratio, and these are shown in Figure 4b and c. For compression ratios between 0.13 and 0.25 (which correspond to q between 0.5 and 2), qcomp/bzip2 is better than hcomp both in RMS difference and in maximum absolute difference. For compression ratios smaller than 0.1 (which correspond to $q > 2$), qcomp is significantly worse than hcomp, first in the RMS difference but eventually also in the maximum absolute difference. This is not surprising, as we saw above that the quantization becomes too coarse for $q > 2$. Thus, in terms of the distribution of differences at a given compression ratio, of the methods we have considered, qcomp/bzip2 is best for compression ratios of 0.13 and above (which corresponds to $q \leq 2$) and hcomp is best for compression ratios smaller than 0.1 (which correspond to $q \geq 4$). The one advantage that hcomp has over qcomp/bzip2 for $q \leq 2$ is that it compresses about three times faster, although both decompress at about the same speed.

At the same value of q (i.e., the same distribution of differences), qcomp/gzip2 produces significantly worse compression ratios then qcomp/bzip2. For example, at $q = 1$ the mean compression ratio of qcomp/gzip is 0.31 compared to 0.19 for qcomp/bzip2. This appears to be not much better than the 0.41 achieved by lossless compression by bzip2, but qcomp/gzip has two advantages: it is roughly four times faster then either lossless bzip2 or lossy qcomp/bzip2, both at compression and decompression, and it achieves more consistent compression ratios than lossless compression.

7. COMPARISON TO OTHER QUANTIZATION METHODS

This section compares the quantization method proposed here, qcomp, to the similar quantization methods proposed by White & Greenfield (1999) and Nieto-Santisteban et al. (1999).

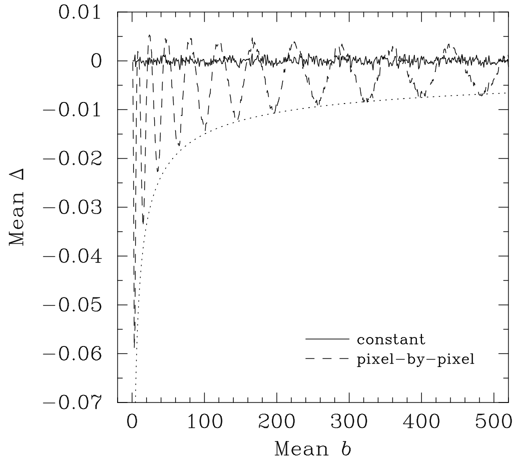

Fig. 5. The mean difference Δ (in units of the noise $\sigma_b = \sqrt{b}$) between the original and quantized images for images quantized with a single quantum for each image and with quanta determined on a pixel-by-pixel basis. The images have a gain of 1 and no read noise, and the quantization has $q = 1$. The dotted line is the approximate lower envelope to the pixel-by-pixel mean difference and has the form $-0.15/\sigma_b$.

7.1. *Distribution of Differences*

White & Greenfield (1999) calculate the quantum from the empirical standard deviation in the image rather than using a noise model. This can cause the actual noise in raw data to be significantly overestimated. Consider the flat field image (e), which has standard deviation of more than 500 (after 3 sigma clipping), but a noise of only about 75. Even if we eliminate the contribution from large-scale structure, the pixel-to-pixel standard deviation is about 160. Obviously, as the empirical standard deviation is larger than the noise, quantizing on the basis of the empirical standard deviation would remove real information on the variations in the flat field. Similar problems can occur in any images with high backgrounds or more generally, in which the empirical standard deviation is not dominated by noise. This comparison is somewhat unfair, in that White & Greenfield (1999) do not claim that their method is suitable for raw data, but it does illustrate the danger of assuming that the noise in an image is related to the empirical standard deviation.

Nieto-Santisteban et al. (1999) quantize by taking the square root of scaled data. This is equivalent to calculating the quantum on a pixel-by-pixel basis and assuming that the read noise is zero. To investigate this, a set of images were created with mean values from 1 to 200 electrons, a gain of 1 electron, no read noise, and with appropriate Gaussian noise (although strictly speaking the noise should be Poissonian), and written with BZERO of 0 and BSCALE of 1. The images were quantized two different ways: first using a single quantum for each image calculated by applying equations 7 and 8 with $q = 1$ to the median pixel value (the quantization method proposed here) and second using individual quanta for each pixel calculated by applying equations 7 and 8 to each pixel value (equivalent to the quantization method suggested by Nieto-Santisteban et al.). The mean differences between the original and quantized images are shown in Figure 5. Quantizing on a pixel-to-pixel basis results in much larger mean differences than using a single quantum, and the differences have an oscillatory structure with a change of gradient every whole integer squared. This probably results from the quantum changing with pixel value, so that the two sides of the distribution of pixel values are quantized slightly differently. The lower envelope appears to be roughly $-0.15/\sigma_b$. The mean difference is small even in the pixel-to-pixel case (of order 1% of the noise for typical signals), but nevertheless quantizing with the same quantum gives a much smaller mean difference (of order 0.05% of the noise).

Thus, it appears that the quantization method proposed here has advantages over the other quantization methods when we consider the fidelity of the compressed image to the original image.

7.2. *Compression Ratio and Speed*

Rice et al. (1993) describe a special-purpose compression algorithm designed to compress low-entropy 16-bit integer data. This method is widely referred to as "Rice compression" and has been used by White & Greenfield (1999), Nieto-Santisteban et al. (1999), and, in a modified form, White & Becker (1998).

The compression ratio achieved by Rice compression appears to be only very slightly better than that achieved by gzip; White & Becker (1998) report 0.255 for Rice and 0.272 for gzip while Nieto-Santisteban et al. (1999) report 0.193 for Rice and 0.202 for gzip (for 2 bits of noise).

White & Becker (1998) report that gzip is "far slower" than their implementation of Rice compression and Nieto-Santisteban et al. (1999) report that gzip is 20 times slower than White's implementation of Rice compression. Both of these articles focus on compressing data on a satellite with only limited computing resources, and so understandably do not consider the speed of decompression. Neither mention the flag given to gzip, but the default is equivalent to "-6" and is about half as fast at compression as "-1". If we assume that the default was used, then Rice compression appears to be about 10 times faster than gzip with the "-1" flag.

It would appear then that the methods proposed by White & Greenfield (1999) and Nieto-Santisteban et al. (1999) would produce similar compression ratios to qcomp/gzip2 but would would compress much more quickly; neither method is likely to produce compression ratios that are as good as those produced by the much slower qcomp/bzip2. Of course, it would be possibly to adapt qcomp to use Rice compression or the other methods to use bzip2, in which case they should produce very similar compression ratios and speeds.

8. DISCUSSION

8.1. *Suitability for Compressing Raw Data*

The quantization compression method described here, qcomp, was designed to compress raw data. With the results of the tests and comparisons in § 6 and § 7, we can now critically evaluate its suitability for this task. We will see that that qcomp is better suited for compressing raw data than either hcomp (White 1992) or the quantization methods proposed by White & Greenfield (1999) and Nieto-Santisteban et al. (1999).

The fundamental advantage of qcomp over hcomp is that its straightforward nature allows firm limits to be placed on the distribution of differences (see § 5). So, for example, an image can be compressed with the knowledge that no pixel will change by more than a specified amount. Furthermore, the distribution of the errors is predictable. Hcomp does not give such firm guarantees on the distribution of differences.

However, this advantage would be moot if qcomp were inferior in compression ratio and speed. The most interesting range of q for compressing raw images is 0.5–2, that is, quantizations that change the values in the image by at most 0.25–1 standard deviations. In this range, qcomp/bzip2 gives mean compression ratios of 0.27–0.13 and gives roughly the same RMS difference as hcomp for similar compression ratios but with smaller maximum absolute differences and mean differences (see Fig. 4). Furthermore, its decompression speed is very similar to hcomp. Its only disadvantage is that its compression speed is only one third that of hcomp, although it is still adequately fast; its compression rate of roughly 800 kpixel/s on a 1.9 GHz Pentium IV is much faster than the typical read rate of 40 kpixel/s for single-output CCDs and 160 kpixel/s for quad-output CCDs.

It is also worth considering qcomp/gzip, which achieves lower compression ratios of 0.38–0.23 for q in 0.5–2, while compressing slightly faster and decompressing very much faster than hcomp. It also has the great advantage of portability; gzip is installed almost universally on workstations.

The current implementation of qcomp has a further small advantage over the current implementation of hcomp in that it distinguishes between the data and overscan sections of an image and quantizes each appropriately; the current implementation of hcomp treats both identically, and so the two have to be separated and compressed individually to avoid either drastic over-compression of the overscan section or under-compression of the data section.

The advantages of the qcomp over the other quantization methods are that the manner in which White & Greenfield (1999) determine the quantization makes their method unsuitable for use with raw data (and indeed such a claim was never made) and the manner in which Nieto-Santisteban et al. (1999) quantize introduces a small bias that is not present with qcomp. When using the same lossless compression method, all of the quantization methods should be similar in speed. The one disadvantage of qcomp is that is requires that the noise in the background be roughly constant within fixed regions, whereas the method of Nieto-Santisteban et al. (1999) estimates the noise on a pixel-by-pixel basis and makes no such requirement. However, this may not be too restrictive as the noise varies only as the square root of the background (and more slowly if read noise is significant), so changes in the background produce much smaller changes in the noise.

Obviously, confidence in the use of qcomp to compress raw data would be significantly improved if end-to-end tests on compressed data gave results that were statistically indistinguishable from those derived from the original data. Such tests should include astrometry of stars, aperture and PSF-fitting photometry of stars, and photometry of low surface brightness sources. These tests are especially important for applications which have stringent requirements on the absence of biases, such as far infrared and sub-millimeter imaging and ultra low surface brightness studies at other wavelengths. Such tests will be presented in Paper II (Watson, in preparation).

8.2. *Distribution*

An important advantage of compressing files with qcomp/gzip is that they can be distributed with the expectation that no additional software will be needed to decompress them; gzip is installed almost universally on workstations. As bzip2 becomes more widespread (it already forms part of several Linux distributions), it too will gain this advantage. This is a major advantage over software that uses special-purpose compression methods.

8.3. *Media Capacities*

If we take a compression ratio of 0.2 as typical for qcomp/bzip2 with $q = 1$, then media have effective capacities that are 5 times larger than their raw capacities. Thus, a 650 MB CD-ROM has an effective capacity of 3 GB, a 12 GB DAT DDS-3 tape has an effective capacity of 60 GB, and an 80 GB disk has a capacity of 400 GB. This is roughly equivalent to a generation of technology; in terms of capacity, a CD-ROM is almost a DVD-ROM, a DAT tape is effectively a DLT tape, and a single disk is effectively a large RAID array. Thus, compression can allow one to work with large data sets without acquiring the devices often considered essential.

8.4. *Bandwidth*

If images can be compressed and decompressed sufficiently quickly, compression increases the effective bandwidth of a device or transport mechanism by a factor equal to the inverse of the compression ratio. Thus, it may be faster to store images in their compressed form, even though there is an overhead in compressing or decompressing them.

Table 4 shows for several devices or transport mechanisms the raw bandwidths and the current and maximum effective bandwidths for compressed data, assuming a compression ratio of 0.3 appropriate for compression with qcomp/gzip with $q = 1$. The maximum bandwidths assume an arbitrarily fast processor, so the overheads of compression and decompression drop to zero. The current read and write bandwidths were measured or estimated for qcomp/gzip on an early-2002 computer with single 1.9 GHz Pentium IV processor, which can compress at about 3 Mpixel/s and decompress at about 12 Mpixel/s. (A similar table could be constructed for qcomp/bzip2; the maximum effective bandwidths would be higher

TABLE 4

DEVICE AND TRANSPORT MECHANISM SPEED

Device	Bandwidth (Mpixel/s)			
	Raw	Current Read	Current Write	Maximum
Slow single disk	4	12	3	13
Fast single disk	7	12	3	23
Fast RAID disk array	25	12	3	83
50× CD-ROM	4	12		13
4× CD-R	0.3		1	1
DAT DDS-3	0.6	2	2	2
DLT	2.5	8	3	8
56 kbps link	0.003	0.01	0.01	0.01
10 Mbps link	0.5	1.7	1.7	1.7
100 Mbps link	5	12	3	17
1 Gbps link	50	12	3	150

and the current effective bandwidths would be lower, except for the 56 kbps link which would have a current effective bandwidth of 0.015 Mpixel/s.)

Table 4 shows that even now compression results in an improvement in effective bandwidth for CD-ROMs, tapes, single disks, and all but the very fastest network connections. As processors become faster, the actual bandwidths will approach the maximum bandwidths, and, for fast enough processors, all devices will benefit. For example, achieving 83 Mpixel/s read bandwidth from a fast RAID array will require processors only 7 times faster than a 1.9 GHz Pentium IV; if processors continue to double in speed every 18 months, according to Moore's law, such processors should be available in about 2006. Achieving 83 Mpixel/s write speed will require processors 28 times faster which should be available in about 2009. Alternatively, if we allow 8-way parallelism (see § 9.2), such speeds should be possible now for reading and in about 2005 for writing. (Again assuming 8-way parallelism, qcomp/bzip2 should give 125 Mpixel/s read bandwidth around 2006 and 125 Mpixel/s write bandwidth around 2008.)

9. POSSIBLE IMPROVEMENTS

9.1. *Compression Ratio*

The compression ratio could be improved by using a compression method that performed better than bzip2. However, the experiments above indicate that bzip2 is better than both optimal 16-bit and optimal 32-bit compression, so this may be difficult.

Furthermore, it is easy to show that bzip2 is performing very close to optimally. The mean compression ratio achieved by qcomp/bzip2 with $q = 1$ is 0.193. The mean compression ratios achieved by bzip2 and optimal 16-bit compression of Gaussian noise with the same q values (which, as mentioned above, are really $q = 0.8$ and $q = 0.7$ for images (a) and (b)) are 0.172 and 0.143. This suggests that a hypothetical compression method that compressed the information as well as bzip2 and compressed the noise as well as optimal 16-bit compression would achieve a compression ratio of about 0.164, an improvement of only 18%. Even a hypothetical compression method that compressed the information to nothing and compressed the noise as well as optimal 16-bit compression would achieve a compression ratio of about 0.143, an improvement of only 35%. It seems that bzip2 is close to optimal, and any further improvements will be small; there are no more factors of two to be gained.

One means to improve the compression ratio in high-background images would be to roughly flatten and/or subtract the sky prior to compression. This should narrow the histogram of pixel values and thereby improve subsequent compression. However, again, there's not much to be gained. The difference between the compression ratios for the bias image (a) and the flat-field image (e) is only 10% for qcomp/bzip2 with $q = 1$; bzip2 is doing a very good job of encoding both the pixel-to-pixel and large-scale structure in the flat-field image, and so would presumably perform similarly well on other high-background images.

9.2. *Speed*

An obvious improvement to the writing speed would be to parallelize the quantization and compression steps. This has already been implemented in qcomp, as the quantized image is piped to the lossless compressor as it is created. The improvements are up to 50% for qcomp/gzip and 10% for qcomp/bzip2.

To obtain further improvements, compression and decompression must be made faster. For both gzip and bunzip2, compression can be trivially parallelized by splitting the input between processes and concatenating the output from each process. Unfortunately, the file formats for gzip and bzip2 do not permit decompression to be parallelized. (The only way to determine the length of a compressed block is decompress it.) However, it would be a simple matter to modify the format of the compressed files to permit decompression to be parallelized (by prefixing each compressed block with its length); this would not be so conveniently portable, but might be worthwhile for private use.

Rice compression might be attractive if more speed is required and compression ratios similar to those of gzip are adequate. That said, even if the cost of lossless compression could be reduced to zero, determining the noise level and quantizing would still require effort and would limit the compression speed to only about 3 times that of qcomp/gzip. (It is possible that the noise level could be determined more rapidly by determining the noise from only a subsample of pixels, in which case the compression speed might improve by a somewhat larger factor).

9.3. *Robustness against Varying Backgrounds*

One problem with the current implementation of qcomp is that it assumes that the whole data section of the image can be adequately characterized by a single background and hence a single background noise. (It does, however, allow the data and bias sections to have different backgrounds.) This will present a problem for images that have very different background levels, for example, spectra in the thermal infrared in which the thermal background increases rapidly with wavelength.

This situation could be improved by subdividing the data section into regions such that each region is adequately characterized by a single background. This could be achieved manually or perhaps adaptively. One adaptive scheme would be to subdivide regions recursively until the backgrounds in the subregions are not significantly different from the background in the region.

Another option would be to estimate the noise and hence the quantum on a pixel-by-pixel basis, following Nieto-Santisteban et al. (1999), but as has been shown this introduces a small bias in the mean difference between the quantized and original images.

10. SUMMARY

A lossy method for compressing raw images has been presented. The method is very simple; it consists of lossy quantization (resampling in brightness) followed by lossless compression. The degree of quantization is chosen to eliminate the low-order bits that over-sample the noise, contain no information, and are difficult or impossible to compress.

The method is lossy but gives certain guarantees about the distribution of differences between the compressed and original images. In particular, it gives guarantees on the maximum absolute value, the expected mean value, and the expected RMS value of the difference. These guarantees make it suitable for use on raw data.

The method consistently reduces images to 1/5 of their original size while changing no value by more than 1/2 of a standard deviation in the background. This is a dramatic improvement on the compression ratios achieved by lossless compression. The method is adequately fast on current computers and would be relatively simple to parallelize.

A key feature of the method is that data can be uncompressed using tools that are widely available on modern workstations, which means that one can distribute compressed data and expect that they can be used without the need to install specialized software. This is achieved by writing the quantized image as a normal FITS file and compressing it with gzip and bzip2, which are widely available general-purpose compression tools. It appears that bzip2 is compressing the data within a few tens of percent of optimally.

The next step in the development of this method is real-world testing with compressed raw data to ensure that the method does not degrade the results of astronomical analyses. Such end-to-end tests will be presented in Paper II (Watson, in preparation).

I thank Enrique Gaztañaga for his referee's report, possibly the most useful I have ever received, and in particular for his suggestion to compare my results to the Shannon entropy limit. I thank Rick White for useful comments on hcomp and for blazing the trail. I thank Julian Seward, Jean-Loup Gailly, Mark Adler, and Markus Oberhumer for doing the hard work of writing bzip2, gzip, and lzop. I thank the staff of the Observatorio Astronómico Nacional de México at San Pedro Mártir for their warm hospitality in February 1999, when the ideas presented here were conceived.

REFERENCES

Beckett, M. G., Mackay, C. D., McMahon, R. G., Parry, I. R., Ellis, R. S., Chan, S. J., & Hoenig, M. 1998, Proc. SPIE, 3354, 431

Gailly, J.-L. 1993 “gzip: The data compression program” (http://www.gzip.org/)

Gaztañaga, E., Romeo, A., Barriga, J., & Elizalde, E. 2001, MNRAS, 320, 12

Huffman, D. A. 1952, Proceedings of the Institute of Radio Engineers, 40, 1098

Louys, M., Starck, J.-L., Mei., S., Bonnarel, F., & Murtagh, F. 1999, A&AS, 136, 579

Nieto-Santisteban, M. A., Fixsen, D.J., Offenberg, J. D., Hanish, R. J., & Stockman, H. S. 1999, in Astronomical Data Analysis Software and Systems VIII, eds. D. M. Mehringer, R. L. Plante, & D. A. Roberts (San Francisco: ASP), 137

Oberhumer, M. F. X. J. 1998, “lzop - compress or expand files” (http://www.oberhumer.com/opensource/lzop/)

Press, W. H. 1992, Astronomical Data Analysis Software and Systems I, eds. D. M. Worrall, C. Biemesderfer, & J. Barnes (San Francisco: ASP), 3

Press, W.H ., Teukolsky, S. A., Vetterling, W. T., & Flannery, B. P. 1992, Numerical Recipes in C (Cambridge: CUP), 2nd edition

Rice, R. F., Yeh, P.-S., & Miller, W. H. 1993, in Proceedings of the 9th AIAA Computing in Aerospace Conference (AIAA-93-4541-CP)

Romeo, A., Gaztanaga, E., Barriga, J., & Elizalde, E. 1999, International Journal of Modern Physics C, 10, 687

Seward, J. R. 1998, “bzip2 and libbzip2: a program and library for data compression” (http://sources.redhat.com/bzip2/)

Shannon, C. E. 1948a, Bell System Technical Journal, 27, 379

__________. 1948b, Bell System Technical Journal, 27, 623

__________. 1949, Proceedings of the Institute of Radio Engineers, 37, 10

Veillet, C. 1998, MegaPrime: A New Prime-Focus Environment and Wide Field Image Camera in CFHT Information Bulletin, 39

Véran, J. P., & Wright, J. R. 1994, in Astronomical Data Analysis Software and Systems III, eds. D. R. Crabtree, R. J. Hanisch, & J. Barnes (San Francisco: ASP), 519 (ftp://www.cfht.hawaii.edu/pub/compfits/)

Wells, D. C., Greisen, E. W., & Harten, R. H. 1981, A&AS, 44, 363

White, R. L. 1992, in Proceedings of the NASA Space and Earth Science Data Compression Workshop, ed. J. C. Tilton (ftp://stsci.edu/software/hcompress/)

White, R. L., & Becker, I. 1998, On-board compression for the HST Advance Camera for Surveys (http://sundog.stsci.edu/rick/acscompression.ps.gz)

White, R. L., & Greenfield, P. in Astronomical Data Analysis Software and Systems VIII, eds. D. M. Mehringer, R. L. Plante, & D. A. Roberts (San Francisco: ASP), 125

Whitten, I. H., Neal, R. M., & Cleary, J. G. 1987, Communications of the ACM, 30, 520

Alan. M. Watson: Instituto de Astronomía, UNAM, Apartado Postal 3–72 (Xangari) 58089 Morelia, Michoacán, México (a.watson@astrosmo.unam.mx).